

# MHD SIMULATIONS OF PENUMBRA FINE STRUCTURE

T. HEINEMANN<sup>1</sup>

Department of Applied Mathematics and Theoretical Physics, Centre for Mathematical Sciences, Wilberforce Road, Cambridge CB3 0WA, United Kingdom

A. NORDLUND

Niels Bohr Institute, University of Copenhagen, Juliane Maries Vej 30, 2100 Copenhagen, Denmark

G.B. SCHARMER

Institute for Solar Physics, Royal Swedish Academy of Sciences, AlbaNova University Center, 10691 Stockholm, Sweden

AND

H.C. SPRUIT

Max Planck Institute for Astrophysics, Box 1317, 85741 Garching, Germany

*To be submitted to ApJ*

## ABSTRACT

We present results of numerical 3D MHD simulations with radiative energy transfer of fine structure in a small sunspot of about 4 Mm width. The results show the development of filamentary structure with nearly field-free gaps, interlaced by concentrations of stronger magnetic field at the interface between the umbra and the outer field-free atmosphere. Calculated synthetic images show dark cores like those seen in the observations. They are the result of an elevated  $\tau = 1$  surface. The magnetic field in these cores is weaker and more horizontal than for adjacent brighter structures at the photosphere. Higher up in the atmosphere there are only small variations in field strength. Movies made show an inward migration of filamentary structures very similar to the patterns seen in observations of the inner penumbra. Although the filamentary structures in the simulations are too short compared to observations, most other aspects of the simulations appear consistent with observed penumbra filamentary structures.

*Subject headings:* sunspots – magnetic field

## 1. INTRODUCTION

Explaining the magnetic field, Evershed flow, overall fine structure of sunspot penumbrae and the observed high heat flux (75% of that of the quiet sun atmosphere), constitute some of the most longstanding problems in solar physics. Despite nearly a century of detailed studies, no consensus has been reached as regards the origin, or even morphology, of this fine structure. A major obstacle to progress is our inability to adequately resolve sunspot fine structure when observations are carried out with spectrographs or spectropolarimeters. The discovery of dark-cored penumbra filaments (Scharmer et al. 2002) suggests that the basic elements of penumbral structure are now observable with imaging instrumentation.

Ambiguities associated with interpretations of existing observational data have given rise to a diversity of models and explanations for flows and fine structure in penumbrae (e.g., Meyer & Schmidt 1968, Solanki & Montavon 1993, Schlichenmaier et al. 1998a,b, Thomas et al. 2002). In contrast to what is the case for granulation (e.g. Stein and Nordlund 1998), faculae (Carlsson et al. 2004, Keller et al. 2004, Steiner 2005) and umbral dots (Schüssler & Vögler 2006), realistic numerical simulations of entire sunspots have not yet been feasible. This is partly due to difficulties of thermally relaxing such a deep structure and maintaining its stability, but mostly due to the huge range of scales associated with a fully developed sunspot.

### 1.1. *The gappy penumbra*

Recently, Spruit and Scharmer (2006, hereafter SS06a) have pointed to a similarity between penumbral filaments and light bridges, the field-free lanes often seen crossing an umbra. Both have a dark core: a narrow dark lane along their mid-line. In SS06a we have argued that this is not just an observational congruence, but actually indicates a common origin for these structures: gaps in the magnetic field, closing near the visible surface, and heated by convection in the gap. In Scharmer and Spruit (2006, hereafter SS06b) magnetostatic models for such structures were presented. Their properties, distinctly different in the inner and outer penumbra, explain a number of observations, such as the differences in strength and inclination of the magnetic field between dark and bright penumbral structure.

Radiative MHD simulations of light bridges by one of the authors (AN, unpublished) and Heinemann (2006) show how the dark cores over the middle of the light bridges are formed. They are found to be a consequence of hydrostatic pressure and radiative energy balance around the ‘cusp’ of the magnetic field, at the height in the atmosphere where field lines from both sides close over the gap. These simulations thus provide a physical explanation for dark cores that strengthens the interpretation of bright penumbral filaments in terms of field-free gaps. A second observational clue is given by umbral dots, which are often seen to evolve from the ‘heads’ of penumbral filaments propagating into the umbra. As proposed by Parker (1979), seen in numerical simulations by Nordlund & Stein (1990), and recently confirmed through high resolution numerical simulations by Schüssler and Vögler (2006),

<sup>1</sup> Previously at: NORDITA, AlbaNova University Center, 10691 Stockholm, Sweden

umbral dots are the surface manifestation of field-free gaps below the umbral photosphere. This theoretical evidence is strengthened observationally by the short dark cores seen to cross peripheral umbral dots (Scharmer et al. 2002).

High-resolution images of complex sunspot groups (e.g., Fig. 1 of Rouppe van der Voort et al. 2004) show penumbra structures associated with both small and large, symmetric and irregular sunspots, and even penumbrae without visible umbrae. This suggests that there is no need to model entire sunspots to explain penumbra fine structure. This, and the rapid formation of penumbrae with well developed Evershed flows (Leka & Skumanich 1998, Yang et al. 2003), also suggest that details of the deep structure of the magnetic field may not be crucial for these structures. In this paper, we describe first results from realistic simulations of penumbra fine structure. The model used for these simulations is a rectangular section of the solar atmosphere containing a part of a sunspot with umbra and penumbra, embedded in an essentially field-free atmosphere. The simulations show the development of short filamentary structures, associated with the formation of gaps with strongly reduced field strength. They resemble observed penumbral filaments as seen in the inner penumbra: like these, they have a characteristic head-and tail structure with a dark core running along the tail, and are seen to propagate inward.

## 2. MHD SIMULATIONS

The simulations were carried out using the PENCIL code<sup>2</sup>, modified to handle energy transfer by radiation in a grey atmosphere (Heinemann 2006, Heinemann et al. 2006). We used a rectangular computational box  $12448 \text{ km} \times 6212 \text{ km}$  in the horizontal directions, extending over a depth range of  $3094 \text{ km}$  and with a grid separation of  $24.36 \text{ km}$  in both horizontal and vertical directions ( $512 \times 256 \times 128$  grid points). The quiet sun photosphere is located approximately  $700 \text{ km}$  below the upper boundary. In the horizontal directions, periodic boundary conditions are used. Both the upper and lower boundaries are closed in the sense of not allowing vertical flows at these boundaries. The magnetic field strength is kept fixed at the lower boundary but is free to evolve at the upper boundary.

The initial magnetic field of the simulations is a potential (current-free) magnetic field, separated by a current sheet from the surrounding convection zone. This magnetic field is defined by two free parameters, the total vertical flux and the ratio of gas pressure to magnetic pressure,  $\beta$ , along the current sheet. For all calculations made,  $\beta$  was assumed to be independent of depth. The corresponding potential field, given by magnetostatic equilibrium with a gas pressure obtained from a convection simulation and the chosen value of  $\beta$ , was calculated with the method described in SS06b. Since the subsequent magnetic field evolution is driven by the internal dynamics of the model, the choice of the total vertical flux and  $\beta$  primarily constrains the width and field strength of the flux bundle close to the lower boundary.

We made several simulations with different values for the total vertical flux and  $\beta$ . All simulations showed the formation of dark-cored filamentary structures, but with variations in their morphology, number density and life times. Here we discuss only the results of one of these simulations, obtained with an average vertical field strength of  $1 \text{ kG}$  and  $\beta=19$ , corresponding to an initial ratio of the gas pressures in the mag-

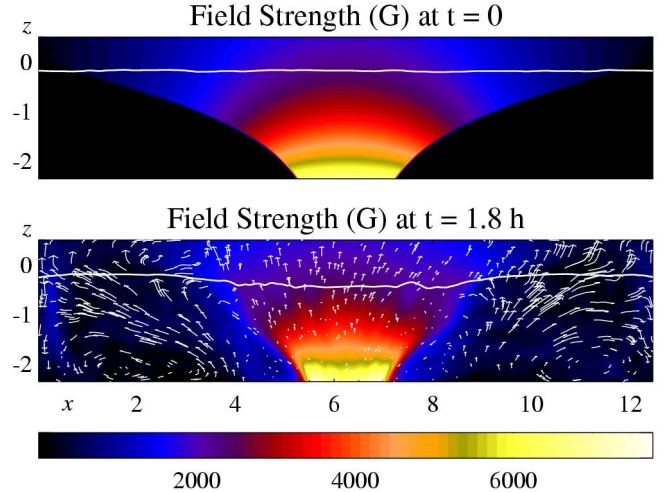


FIG. 1.— Magnetic field strength for the initial state (upper panel) and averaged over time for the evolved model (lower panel). The lower panel also shows the average flow field (arrows). Also shown is a contour at constant optical depths  $\tau = 1$ .

netic to photospheric gas pressures of  $\beta/(\beta + 1) = 0.95$ . The initial magnetic field configuration is shown in Fig. 1 (upper panel).

The temperature, gas pressure, and velocity field were initialized from a field-free convection simulation. The gas pressure in the magnetic atmosphere was then reduced by multiplication of the mass density by  $\beta/(\beta + 1)$  and the magnetic field was added to the model. The strong suppression of convection by the magnetic field causes a rapid drop in temperature, leading to a strong reduction in gas pressure above the umbra and hence a partial collapse of the magnetic field configuration. After approximately 20 solar minutes, the gas reached a quasi-equilibrium state. The magnetic field strength and flow field (arrows) after approximately 1.8 solar hours, averaged over the  $y$ -direction, is shown in Fig. 1 (lower panel).

We assumed a 6th order hyperdiffusivity of  $2 \cdot 10^{-9}$  and a shock diffusivity of 5 (cf. Eqs. (130) and (44) of the PENCIL code documentation—see the footnote), in units where length is measured in megameters and time is measured in kiloseconds. The hyperdiffusivity is adequate to avoid the development of ripples at the grid scale, while leaving larger structures essentially inviscid and non-resistive. The shock diffusivity ensures that shocks—which are ubiquitous in the upper photosphere—are adequately resolved by the difference scheme. Radiative energy transfer was handled using 6 rays along the coordinate axes in most cases. A few tests were made where rays along the space diagonals were added; no major differences were noticed.

## 3. RESULTS

### 3.1. Dark-cored filamentary structures

Following the initial dramatic adjustment of the model to the applied magnetic field, convection in the field-free gas forms small intrusions into the magnetic atmosphere, propagating towards the umbra. Dark lanes, similar to the dark cores of penumbral filaments (Scharmer et al. 2002), form rapidly. A stable situation is reached, where filaments continuously form and disappear on time scales on the order of 10 minutes.

<sup>2</sup> see <http://nordita.dk/software/pencil-code>

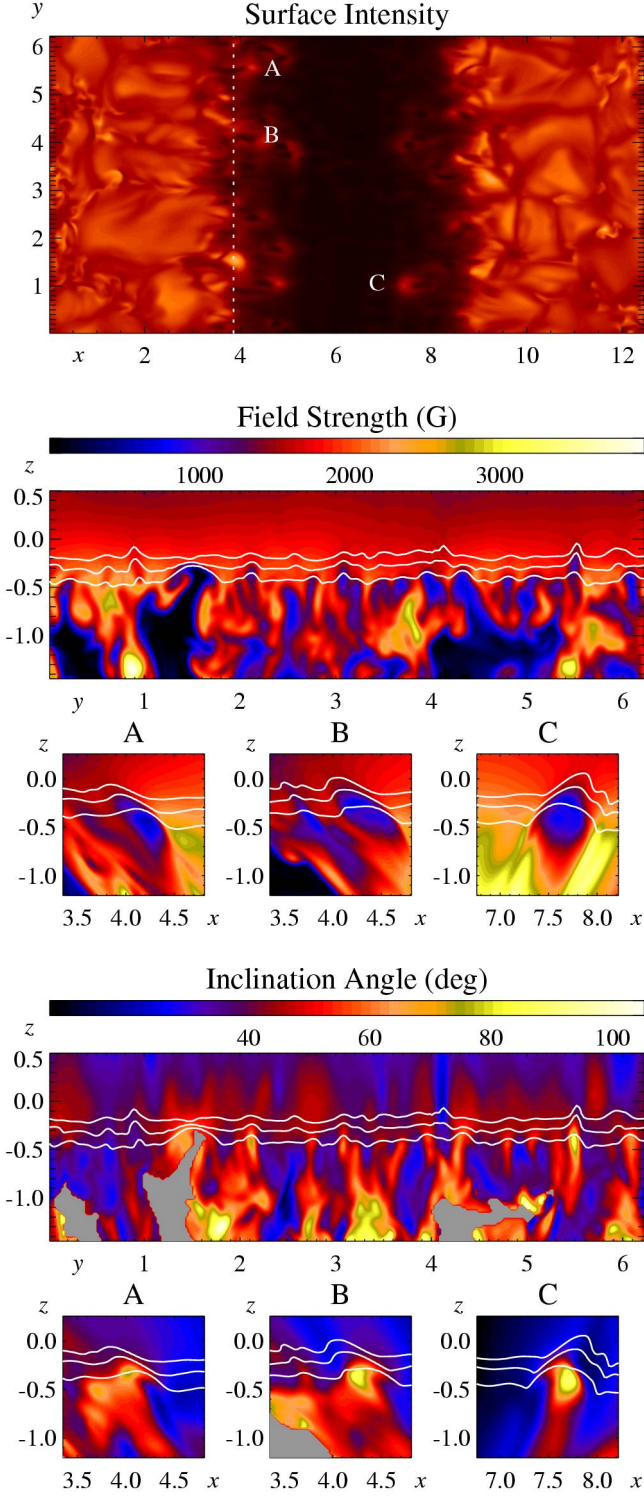


FIG. 2.— Emergent intensity and false-color images of the magnetic field strength and inclination along the dotted line in the intensity image. The six small panels show the field strength and inclination for cuts along three dark-cored filamentary structures (indicated A-C) in the direction perpendicular to the dotted line. Tickmarks and axis labels indicate units in Mm.

Figure 2 shows a snapshot after 1.5 solar hours of the emergent intensity and the field strength for a vertical slice of the model at the location of the dotted line in the intensity image.

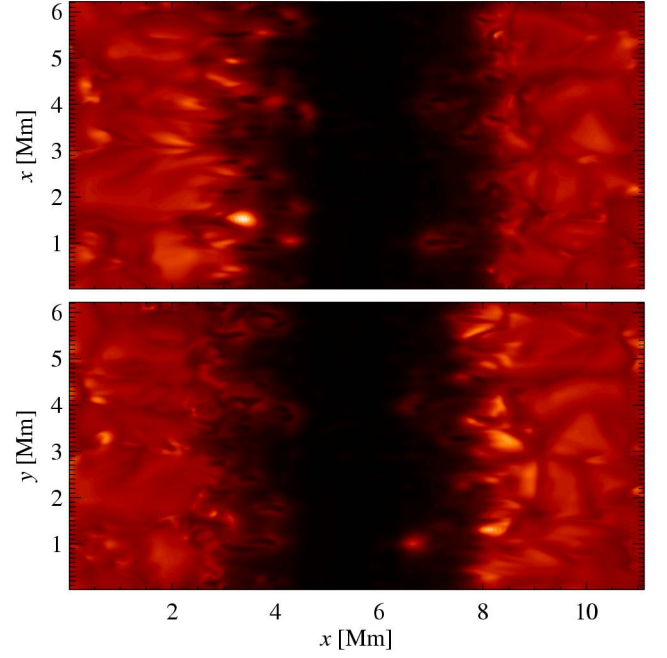


FIG. 3.— Calculated synthetic images corresponding to a heliocentric distance of  $45^\circ$ . In the top image, the limb direction is left, in the bottom image the limb direction is right. To facilitate comparison with the corresponding disk-center image (fig. 2), the fore-shortening of the image in the horizontal direction has been compensated.

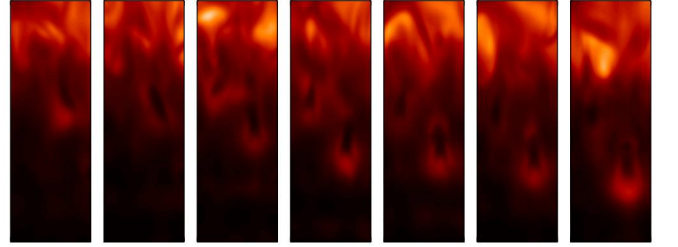


FIG. 4.— Evolution and inward migration of the dark-cored structure labeled ‘C’ in Fig. 2 during 10 solar minutes. The last snapshot is from the larger field-of-view shown in Figs 2 and 3.

Shown in the intensity image, are several short dark-cored filamentary structures protruding into the umbra. The cross-section of the field strength shows several field-free gaps near the visible surface, while below the surface the magnetic field is strongly fragmented with many and extensive field-free gaps. In Fig. 2 is shown also the magnetic field strength and inclination of four dark-cored filaments along cuts perpendicular to the dotted line in the intensity image. These cuts show nearly field-free intrusions that extend over approximately 400 km in depth only and that appear similar to the field-free gaps in the umbral dot simulations of Schüssler and Vögler (2006). These cuts also demonstrate that the gaps are tilted and roughly aligned with the surrounding magnetic field and that the field is much more horizontal at locations of these filamentary structures than in the surroundings. Shown in Fig. 2 are also contours of constant optical depth for  $\tau = 0.01$ , 0.1 and 1 (top to bottom). Three of the dark-cored filaments are associated with  $\tau = 1$  surfaces that are locally elevated by approximately 100–200 km, implying a strongly localized warped visible surface. At heights of only 100–200 km above



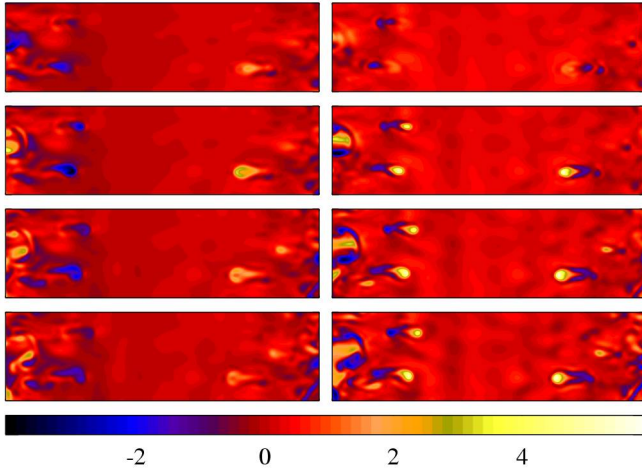


FIG. 5.— Horizontal (left) and vertical velocities at  $z=-0.23$ ,  $-0.35$ ,  $-0.47$  and  $-0.60$  (top to bottom) for the two dark-cored structures on opposite sides of the umbra in Fig. 2.

the  $\tau = 1$  layer, the magnetic field is largely homogeneous, with only small horizontal variations in field strength.

In Fig. 3 is shown the calculated emergent intensities corresponding to a heliocentric distance of  $45^\circ$ . The images show dark-cored structures that are more easily recognized on the disk center side than the limb side but with an overall higher contrast on the limb side. On the limb-side, but not on the disk-center side, at least five round, umbral dot-like structures are seen to connect to dark-cored filaments. These differences between the limb side and disk center side of penumbrae are in excellent qualitative agreement with observations (Sütterlin et al. 2004, Langhans et al. 2006). The explanation for the enhanced visibility of bright dots on the limb side is essentially the same ‘limb brightening’ effect seen in faculae: the line of sight is more perpendicular to the  $\tau = 1$  surface on the limb side, allowing us to see deeper into the hotter layers of the convecting gas (Spruit 1976, Carlsson et al. 2004, Keller et al. 2004).

Movies of the synthetic intensity images show dark-cored filamentary structures forming and migrating toward or into the umbra. Several of these structures are significantly fainter than observed penumbral filaments, resembling instead the faint dark-cored structures described by Scharmer et al. (2002). Figure 4 shows snapshots taken at intervals of 200 s for one such faint dark-cored filament (labeled ‘C’ in Fig. 2), demonstrating the development of a dark core and the inward migration of the structure. During the time interval of 20 solar minutes shown in this figure, this structure propagates approximately 850 km toward the umbra, corresponding to a propagation speed of  $0.7 \text{ km s}^{-1}$ . This is similar to the inward propagation speeds of approximately  $0.5\text{--}1 \text{ km s}^{-1}$  found by Rimmele and Marino (2006) and the  $300 \text{ m s}^{-1}$  found by Langhans et al. (2006).

### 3.2. Flows associated with dark-cored filaments

Figure 5 shows horizontal (left panels) and vertical (right panels) maps of flow velocities at  $z=-0.23$ ,  $-0.35$ ,  $-0.47$  and  $-0.60$  (top to bottom) Mm for two dark-cored filamentary structures shown in Fig. 2. These flow maps show strong upflows in the dot-like brightening and weaker downflows outward of the strong upflow, clearly demonstrating evidence for overturning convection within the field-free gap. This is in sharp

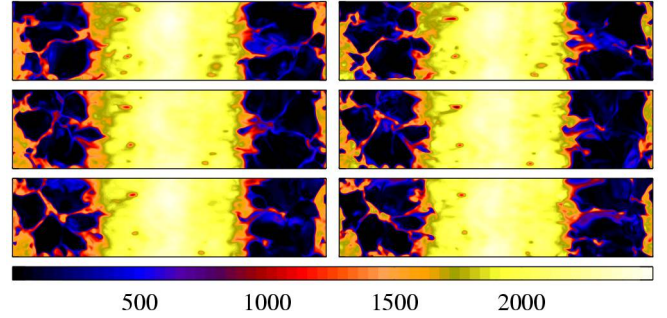


FIG. 6.— Time sequence illustrating the moat flow. The panels (size  $12 \times 3 \text{ Mm}$ ) show the magnetic field strength in  $xy$ -planes at time intervals of 200 seconds. The frames are ordered top-left, top-right, ..., bottom-right.

contrast to a (siphon) flow within a flux tube, where the flow is uni-directional. In the upper layer at  $z=-0.35$ , the magnitude of the upflow is strongly reduced whereas the horizontal outflow peaks at that height. The dark cores are thus associated with flows that are roughly horizontal and aligned with the dark core. Such flows along dark cores were found also in the umbral dot simulations by Schüssler and Vögler (2006). Because of the short horizontal extent of the horizontal flows seen in the present simulations, it is unclear whether we can associate these flows with observed Evershed flows along dark-cored filaments, reported by Rimmele and Marino (2006) and Langhans et al. (2006).

### 3.3. Moat flows

Figure 1 shows an accumulation of magnetic flux at the boundaries of the computational box and also in the deeper layers below the non-magnetic atmosphere. This accumulation of flux is in part due pumping down of the high- $\beta$  magnetic gas by convection below the photosphere and in part due to a large-scale circulation pattern, shown by arrows in the lower panel. Movies of the magnetic field strength near the photosphere show a continuous shredding of magnetic flux from the sunspot and an outward movement of these structures; a time sequence is shown in Fig. 6. This is very similar to observations of moving magnetic features and the moat flow observed in continuum and G-band movies.

## 4. DISCUSSION AND CONCLUSIONS

The present simulations, though of restricted scope, already demonstrate that (nearly) field-free gaps in the penumbra do form, as inferred from the observations by SS06a. The presence of up-flows as well as down-flows within the field-free gaps shows that these gaps are associated with overturning convection, rather than uni-directional (siphon) flows. The structures found in the simulations have several properties in common with observed filaments. They propagate into the umbral magnetic field, and have a dark core overlying the middle. The inward facing head of the structure looks similar to the tip of a filament, as observed at the boundary between umbra and penumbra. The magnetic field in the simulations shows strong fluctuations of the magnetic field inclination across dark-cored filaments. These variations agree with a number of independent observations (see discussion in SS06a and references therein). The dark-cored structures also are associated with horizontal outflows that appear similar to Evershed flows, but because of the short horizontal extent of these

flows, this association remains somewhat unclear. Synthetic images calculated for a heliocentric distance of  $45^\circ$  show distinct differences between the limb side and disk center side that agree with observations: the presence of bright dot-like features on the limb side (but not disk center side), connecting to dark-cored filaments, the better visibility of dark-cored filaments on the center side in spite of a higher overall contrast on the limb side (Sütterlin et al. 2004, Langhans et al. 2006).

In other respects, the structures appearing in the simulations are not yet realistic. They are quite short, and resemble the structure observed near the umbra/penumbra boundary more than the penumbra itself. This may be due to the shallow depth and limited horizontal extent of the computational box. The lower boundary condition used, which keeps the field fixed there, possibly restricts the horizontal extent of developing structure to something comparable with the depth of the box. This could be tested with changes in the lower magnetic boundary condition or its depth.

Another possible cause is that the simulated sunspot, having an umbra with approximately 4 Mm (linear) diameter, has too little magnetic flux to develop a penumbra. This possibility is suggested by observations, which occasionally show pores with diameters as large as 7 Mm without penumbrae (Bray and Loughhead 1964). A contributing factor could be the periodic boundary condition of the simulation in the ‘radial’ direction, which is equivalent to having umbrae of the same polarity next to each other. In observations of neighboring spots of the same polarity, the penumbra is usually suppressed on the side facing the neighboring spot. This may also be the reason why the simulations do not seem to develop something resembling an Evershed flow. The ‘siphon’ mechanism for the Evershed flow, for example (Meyer and Schmidt 1968) relies on the penumbral field lines dipping back into the photosphere not too far from the spot.

Another difference between the simulations and observations concern the lifetimes of the filamentary structures. Observations indicate lifetimes on the order of 1-2 hours, whereas the filaments simulated form and disappear within a typical time span of 10 minutes.

We conclude that the approach to modeling sunspot fine structure by restricting the computational box to a rectangular section of a spot is a viable approach to deal with the huge range of scales associated with a mature sunspot. A number of improvements of these simulations are desirable, some of these are feasible without large increases in computing time. In particular, we will in future simulations increase the size of the computational box in the direction of the magnetic field, to allow sections of larger sunspots to be simulated. The grid separation needs to be reduced in order to adequately resolve the strong vertical gradients associated with radiative cooling in the surface layers and also to represent more accurately the small horizontal scales of the simulated filamentary structures. Another obvious improvement concerns the radiative energy transfer, in the present calculations assumed to be grey and represented by a small number of rays only. A binned opacity treatment, and an increased number of rays should be employed in future experiments.

Finally, Doppler and Stokes spectra calculated from the simulation data will allow ‘forward modeling’ and direct comparisons with dopplergrams and magnetograms.

TH thanks Nordita for financial support and Axel Brandenburg and Wolfgang Dobler for extensive discussions relating to implementation of boundary conditions. Computing time provided by the Danish Center for Scientific Computing (DCSC) is gratefully acknowledged.

#### REFERENCES

- [Bray, R. J., & Loughhead, R. E. 1964, The International Astrophysics Series, London: Chapman Hall, 1964
- [Carlsson, M., Stein, R. F., Nordlund, Å., & Scharmer, G. B. 2004, *ApJ*, 610, L137
- [Heinemann, T., 2006, Master’s Thesis, Niels Bohr Institute, University of Copenhagen
- [Heinemann, T., Dobler, W., Nordlund, Å., Brandenburg, A. 2006, *A&A*, 448, 731
- [Keller, C. U., Schüssler, M., Vögler, A., & Zakharov, V. 2004, *ApJ*, 607, L59
- [Langhans, K., Scharmer, G. B., Kisman, D., Löfdahl, M. G., & Berger, T. E. 2005, *A&A*, 436, 1087
- [Langhans, K., Scharmer, G. B., Kisman, D., Löfdahl, M. G., 2006, *A&A*, submitted
- [Leka, K. D., & Skumanich, A. 1998, *ApJ*, 507, 454
- [Meyer, F., & Schmidt, H. U. 1968, *Mitteilungen der Astronomischen Gesellschaft Hamburg*, 25, 194
- [Meyer, F., Schmidt, H. U., & Weiss, N. O. 1977, *MNRAS*, 179, 741
- [Nordlund, Å., Stein, R. F. 1990, *Proc. IAU Symp.* 138 (ed. J. O. Stenflo), Kluwer, 191
- [Parker, E. N. 1979, *ApJ*, 234, 333
- [Rimmele & Marino(2006)]2006ApJ...646..593R Rimmele, T., & Marino, J. 2006, *ApJ*, 646, 593
- [Roupe van der Voort, L. H. M., Löfdahl, M. G., Kisman, D., & Scharmer, G. B. 2004, *A&A*, 414, 717
- [Scharmer, G. B., Gudiksen, B. V., Kisman, D., Löfdahl, M. G., & Roupe van der Voort, L. H. M. 2002, *Nature*, 420, 151
- [Scharmer, G. B., & Spruit, H. C. 2006, *A&A*, in press
- [Schlichenmaier, R., Jahn K., Schmidt H. U., 1998a, *ApJ*, 493, L121
- [Schlichenmaier, R., Jahn K., Schmidt H. U., 1998b, *A&A*, 337, 897
- [Schüssler, M., & Vögler, A. 2006, *ApJ*, 641, L73
- [Solanki, S. K. 2003, *A&A Rev.*, 11, 153
- [Solanki, S. K., & Montavon, C. A. P. 1993, *A&A*, 275, 283
- [Spruit, H. C. 1976, *Solar Phys.*, 50, 269
- [Spruit, H. C., & Scharmer, G. B. 2006, *A&A*, 447, 343
- [Stein, R. F., & Nordlund, A. 1998, *ApJ*, 499, 914
- [Steiner, O. 2005, *A&A*, 430, 691
- [Sütterlin, P., Bellot Rubio, L. R., Schlichenmaier, R., 2004, *A&A*, 424, 1049
- [Thomas, J. H., Weiss, N. O., Tobias, S. M., & Brummell, N. H. 2002, *Nature*, 420, 390
- [Yang, G., Xu, Y., Wang, H., & Denker, C. 2003, *ApJ*, 597, 1190